

# A Human Hematopoietic Niche Model Supporting Hematopoietic Stem and Progenitor Cells In Vitro

Maaïke V. J. Braham, Amélie S. P. Li Yim, Jara Garcia Mateos, Monique C. Minnema, Wouter J. A. Dhert, F. Cumhur Öner, Catherine Robin, and Jacqueline Alblas\*

Niches in the bone marrow regulate hematopoietic stem and progenitor cell (HSPC) fate and behavior through cell–cell interactions and soluble factor secretion. The niche-HSPC crosstalk is a very complex process not completely elucidated yet. To aid further investigation of this crosstalk, a functional in vitro 3D model that closely represents the main supportive compartments of the bone marrow is developed. Different combinations of human stromal cells and hydrogels are tested for their potential to maintain CD34<sup>+</sup> HSPCs. Cell viability, clonogenic hematopoietic potential, and surface marker expression are assessed over time. Optimal HSPC support is obtained in presence of adipogenic and osteogenic cells, together with progenitor derived endothelial cells. When cultured in a bioactive hydrogel, the supportive cells self-assemble into a hypoxic stromal network, stimulating CD34<sup>+</sup>CD38<sup>+</sup> cell formation, while maintaining the pool of CD34<sup>+</sup>38<sup>−</sup> HSPCs. HSPC clusters colocalize with the stromal networks, in close proximity to sinusoidal clusters of CD31<sup>+</sup> endothelial cells. Importantly, the primary in vitro niche model supports HSPCs with no cytokine addition. Overall, the engineered primary 3D bone marrow environment provides an easy and reliable model to further investigate interactions between HSPCs and their endosteal and perivascular niches, in the context of normal hematopoiesis or blood-related diseases.

## 1. Introduction

The bone marrow is a complex environment in which hematopoietic stem and progenitor cells (HSPC) are maintained in a dynamic balance of quiescence, self-renewal, and differentiation into myeloid, lymphoid, and erythroid lineages.<sup>[1,2]</sup> This dynamic balance is regulated by specialized microenvironments within the adult bone marrow, so called niches, which provides signals to the residing HSPCs.<sup>[3,4]</sup> The HSC niche is formed by two main components: a noncellular component consisting of extracellular matrix (ECM) and soluble factors, and a cellular component constituted by both hematopoietic and non-hematopoietic cells such as endothelial cells, osteoblasts, mesenchymal progenitor cells, and adipocytes.<sup>[5]</sup> The HSC niche is also a physiological hypoxic microenvironment,<sup>[6]</sup> where hypoxia-induced signals are involved in the maintenance of HSC quiescence and survival.<sup>[7]</sup>

Essential cellular components of the HSC niches are mesenchymal progenitors and endothelial cells expressing the chemokine CXCL12; its receptor CXCR4 is essential for the differentiation of multipotent hematopoietic progenitors.<sup>[8]</sup> Multipotent progenitors are believed to be either intermingled with HSCs in the same niche, or residing in a close but distinct niche.<sup>[2]</sup> Their exact location and the existence of separate subniches remain under debate. The two most suggested subniches are the endosteal and the perivascular niche, which are distinguished by differences in cell populations and chemotactic gradients.<sup>[9,10]</sup> The endosteal niche is located at the interface between trabecular bone and bone marrow, and primarily contains osteoblasts.<sup>[11]</sup> The perivascular niche contains sinusoidal endothelium and thus primarily endothelial cells. Quiescent HSCs have been identified near the perivascular niche, while early lymphoid progenitors have been identified closer to the endosteal niche.<sup>[12]</sup>

Established in vitro HSPC niche models use stromal cell lines to provide essential niche signals to the HSCs, and/or by supplementing the used media with high concentrations of growth factors.<sup>[13–17]</sup> HSPCs can be maintained and expanded in vitro for weeks using cytokines, or for longer using feeder cell lines.<sup>[18]</sup> These 2D cultures lack the in vivo niche residing cells that are unmodified through irradiation or transduction,

Dr. M. V. J. Braham, A. S. P. Li Yim, J. Garcia Mateos, Prof. F. C. Öner, Dr. J. Alblas

Department of Orthopaedics  
University Medical Center Utrecht  
Heidelberglaan 100, 3584 CX Utrecht, The Netherlands  
E-mail: j.alblas@umcutrecht.nl

Dr. M. V. J. Braham, A. S. P. L. Yim, J. Garcia Mateos, Dr. C. Robin, Dr. J. Alblas

Regenerative Medicine Center  
University Medical Center Utrecht  
Uppsalalaan 8, 3584 CT Utrecht, The Netherlands

Dr. M. C. Minnema  
Department of Hematology  
University Medical Center Utrecht Cancer Center  
Heidelberglaan 100, 3584 CX Utrecht, The Netherlands

Prof. W. J. A. Dhert  
Faculty of Veterinary Medicine  
Utrecht University  
Yalelaan 7, 3584 CL Utrecht, The Netherlands

Dr. C. Robin  
Hubrecht Institute-KNAW  
University Medical Center Utrecht  
Uppsalalaan 8, 3584 CT Utrecht, The Netherlands

 The ORCID identification number(s) for the author(s) of this article can be found under <https://doi.org/10.1002/adhm.201801444>.

DOI: 10.1002/adhm.201801444

as well as the 3D environment and ECM components of the natural HSC niche. The ECM has been shown to have an important role within the stem cell niche, as it can directly or indirectly modulate the maintenance, proliferation, self-renewal, and differentiation of stem cells.<sup>[19]</sup> Also the natural residing cells are of high importance to study both normal and disordered development of HSCs. Altered signaling in osteocytes causes myeloid hyperproliferation, whereas alterations in mesenchymal osteoprogenitors in the bone marrow result in myelodysplastic syndrome and the development of acute myeloid leukemia.<sup>[20,21]</sup> Mimicking the various elements of the HSC niche would enable the study of the niche itself, and its active participation in normal hematopoiesis as well as in the context of disease pathogenesis.

Various studies have been conducted aiming to develop in vitro models capable of supporting HSPCs in a 3D environment. When developing an in vitro HSPC model, it is of importance to optimize both the cellular compartment of the model, as well as the used hydrogel mimicking the ECM of the niche. To mimic the endosteal niche, hydrogels (e.g., Matrigel, collagen, Puramatrix, alginate, or PEG)<sup>[22–26]</sup> or bone mimicking materials (e.g.,  $\beta$ TCP, hydroxyapatite, or bioderived bone)<sup>[24,27–29]</sup> have been used. In addition to these materials, models used either stromal cell lines<sup>[22,30,31]</sup> or human primary cells as supportive cell sources. The primary cell sources are multipotent mesenchymal stromal cells (MSCs) or osteogenic differentiated MSCs (O-MSCs).<sup>[24–29,32–37]</sup> In these primary cell models, the use of additional cytokine supplemented medium is still common practice, to enhance the survival of the cultured HSPCs. This suggests suboptimal support of the used primary cells toward the cultured HSPCs. Endothelial cells and perivascular stromal cells are cell types known to be critical for the production of HSC niche factors.<sup>[12,38]</sup> Also adipocytes were shown in vitro to suppress HSPC differentiation and support their survival.<sup>[39]</sup> However, none of the developed models included either endothelial cells or adipocytes. Through optimization of the supporting primary cells, supplementation of cytokines would ideally no longer be necessary, as these soluble factors would then be produced by the fabricated supportive tissue. A model with higher cellular complexity would also enable research on the role of various niche residing cell types in the regulation and support of HSPCs, as well as disease pathogenesis.

The aim of this study was to identify the potential of various primary cell types to support HSPCs in vitro, without the need of additional cytokines. Also, the efficacy of a bioactive (Matrigel) and bioinert hydrogel (alginate) was tested. The developed 3D coculture model was further characterized, investigating the added value of cytokine supplementation on HSPC support, and the presence of hypoxia within the engineered HSPC niche.

## 2. Results

### 2.1. 3D Culture in Alginate and Matrigel Allows the Survival of MSCs, EPCs, and HSPCs

Selected hydrogels were tested for cell biocompatibility. GelMA, alginate, and Matrigel were tested as they are all known to

homogeneously incorporate cells, while still enabling diffusion of nutrients and metabolites. MSCs were highly viable up to 7 d of culture in all tested hydrogels (Figure 1A). Endothelial progenitor cells (EPCs) remained highly viable after 7 d of culture in Matrigel. Alginate and gelMA cultures resulted in lower EPC viability. HSCP viability was decreased following gelMA encapsulation at day 7, which was not seen with alginate or Matrigel. The bioactive or bioinert nature of the hydrogel was observed after 7 d of culture by looking at cell morphology (Figure 1B). Alginate and Matrigel were both selected for further experiments since they did not affect HSPC viability, and offered the possibility to compare bioactive and bioinert material. Alginate can be decrosslinked after culture, making cell collection for further analysis possible. While Matrigel can be digested using dispase, it also partly digests extracellular cell surface receptors and therefore surface marker expression. To circumvent this issue, a cell recovery solution was used to depolymerize the Matrigel without affecting cell surface receptors (Figure 1C).

### 2.2. The Combination of A-MSCs, O-MSCs, and EPCs in 3D Cocultures Maintains CFU-GEMM Progenitors In Vitro

To create an optimal in vitro bone marrow niche model for HSPC maintenance, varying primary cell sources were combined and tested in 3D alginate plugs (Figure 2; see the Experimental Section for details on the culture conditions). MSCs and EPCs, or a mix of both cell types, enhanced the survival of HSPCs when compared to the culture with no feeder. However, the support was not better when compared to MS-5 cells cocultured with HSPCs. Combined MSCs and EPCs showed a higher supportive trend over time than MSCs or EPCs alone (Figure 2A). MSCs differentiated toward adipocytes (A-MSC) or osteoblasts (O-MSC) showed comparable supportive potential to MS-5, both in the presence or absence of EPCs (Figure 2B). The combination of A-MSCs, O-MSCs, and EPCs enhanced the total number of colonies (mainly BFU-Es) produced at day 3 and 7 compared to MS-5 (Figure 2C). Importantly, the number of CFU-GEMM progenitors was maintained after 10 d of coculture. The adipogenic or osteogenic lineage commitment of A-MSCs and O-MSCs was confirmed before use in the 3D cocultures (Figure 2D).

### 2.3. Matrigel Promotes the Proliferation of HSPCs in Presence of A-MSCs, O-MSCs, and EPCs

The proliferation of HSPCs was tested after cocultured in absence or presence of feeders (i.e., MSCs/EPCs, A-MSCs/O-MSCs/EPCs, MS-5) in either alginate or Matrigel. No differences were observed between the two hydrogels in the absence of feeder cells, or in the presence of MSCs/EPCs. Higher numbers of hematopoietic cells (HCs) were observed in Matrigel cultures at day 7 and 10 in the presence of either MS-5 or A-MSCs/O-MSCs/EPCs (Figure 3A–D). When analyzing surface marker expression, more CD34<sup>+</sup> HSPCs were retrieved from the Matrigel cultures at day 7 compared to day 1, with a significant increase in CD34<sup>+</sup>CD38<sup>+</sup> cells

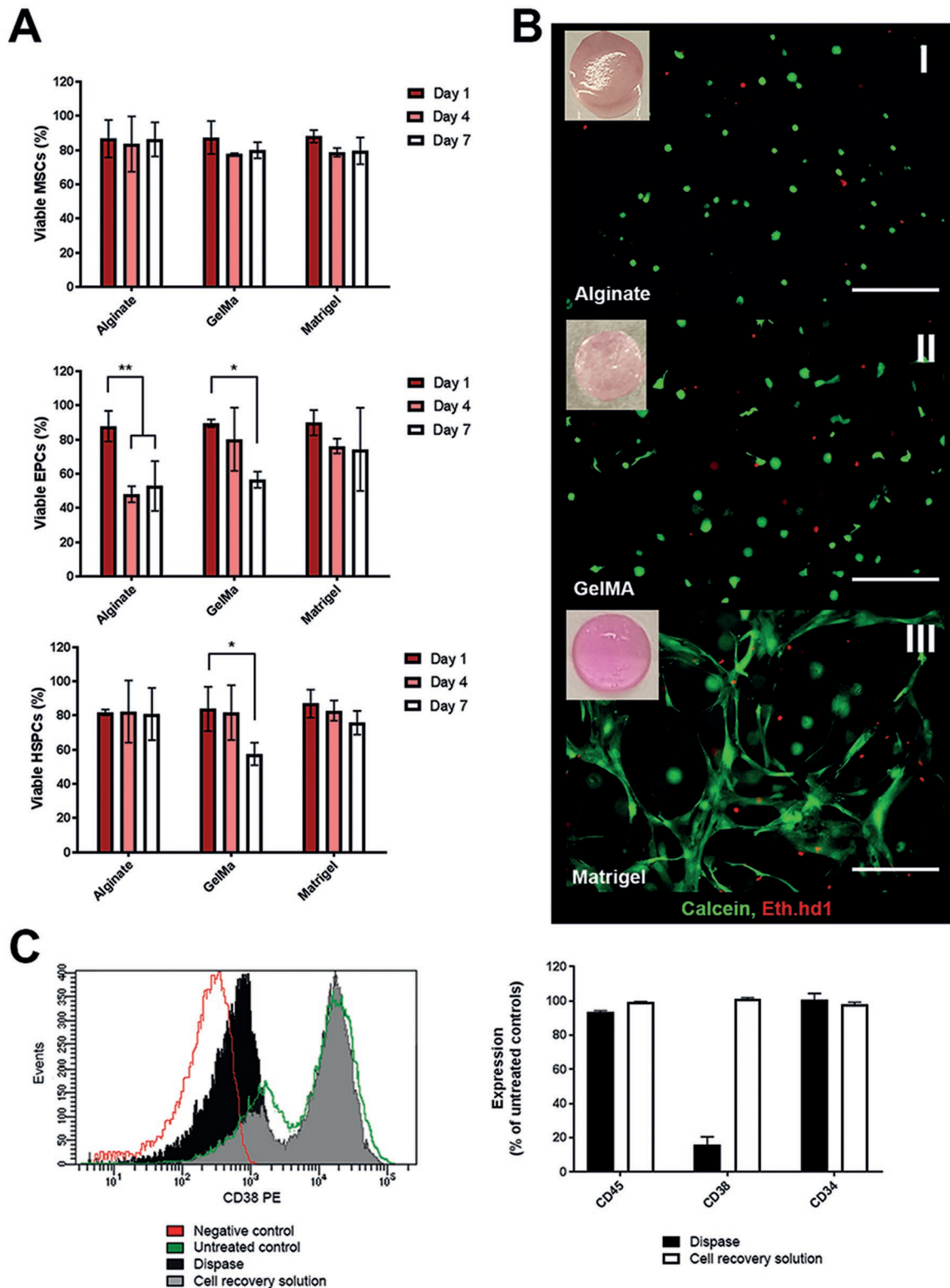


**Figure 1.** Cell viability in various hydrogel matrices and subsequent retrieval from Matrigel. **A**) Cell viability of MSCs, EPCs, and HSPCs (cultured on supportive MS-5 layers) in different 3D hydrogel cultures over time. The live/dead ratio of each cell type ( $n = 3$ ) was analyzed after 1, 4, and 7 d of culture. **B**) Fluorescent images of live (green, calcein) and dead (red, ethidium homodimer-1) MSCs after 7 d encapsulation in different gels (alginate  $20 \text{ mg mL}^{-1}$ , gelMA  $50 \text{ mg mL}^{-1}$  and Matrigel 50% (v/v)). **C**) CD38 (left, flow cytometry) and corresponding CD45, CD38, and CD34 expression percentages (right) of HSPCs recovered from Matrigel at day 7, using either dispase or cell recovery solution. Data are presented as mean  $\pm$  SD. The scale bars represent  $200 \mu\text{m}$ .

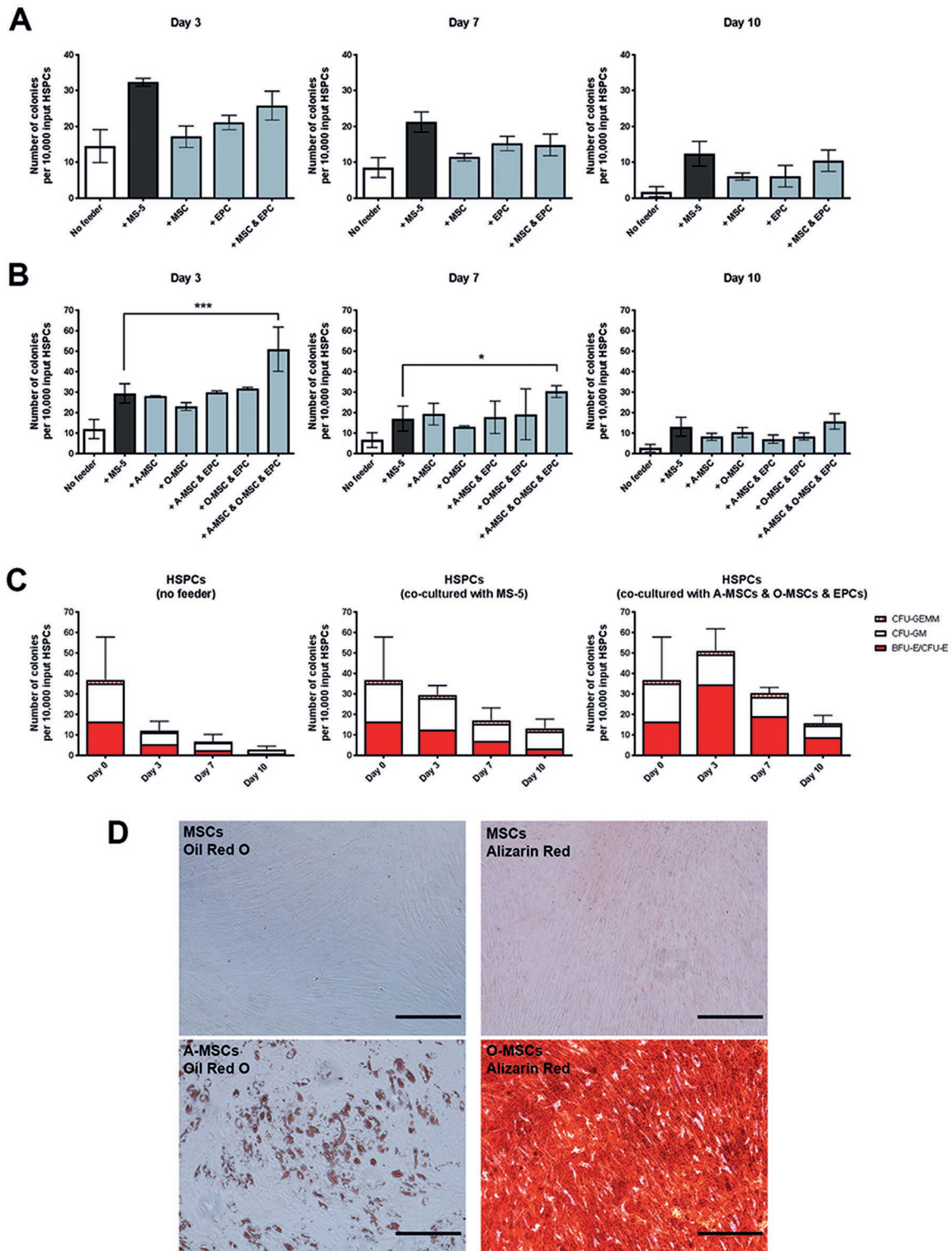


**Figure 2.** Colony-forming potential of HSPCs cultured in various primary coculture conditions, retrieved from 3D alginate plugs. The number of colonies ( $n = 4$ ) was counted before (day 0) and after 3, 7, and 10 d of (co)culture. A) Colony-forming potential of 3D cultured HSPCs without feeder, with MS-5, undifferentiated MSCs, EPCs, or MSCs/EPCs after 3, 7, and 10 d. B) Colony-forming potential of 3D cultured HSPCs without feeder, with MS-5, differentiated A-MSCs, O-MSCs, or cocultured A-MSCs/EPCs, O-MSCs/EPCs, or A-MSCs/O-MSCs/EPCs after 3, 7, and 10 d. C) Type of colonies (CFU-GEMM, CFU-GM, and BFU-E/CFU-E) generated after the 3D culture with no feeder, MS-5, and A-MSCs/O-MSCs/EPCs. D) Bright field images of MSCs cultured for 14 d in MSC medium, osteogenic medium, or adipogenic medium. MSCs were stained with Oil Red O or Alizarin Red to identify lipid formation or mineralized matrix, respectively. Data are presented as mean  $\pm$  SD. \*  $p < 0.05$ , \*\*\*  $p < 0.001$ . The scale bars represent 200  $\mu$ m.

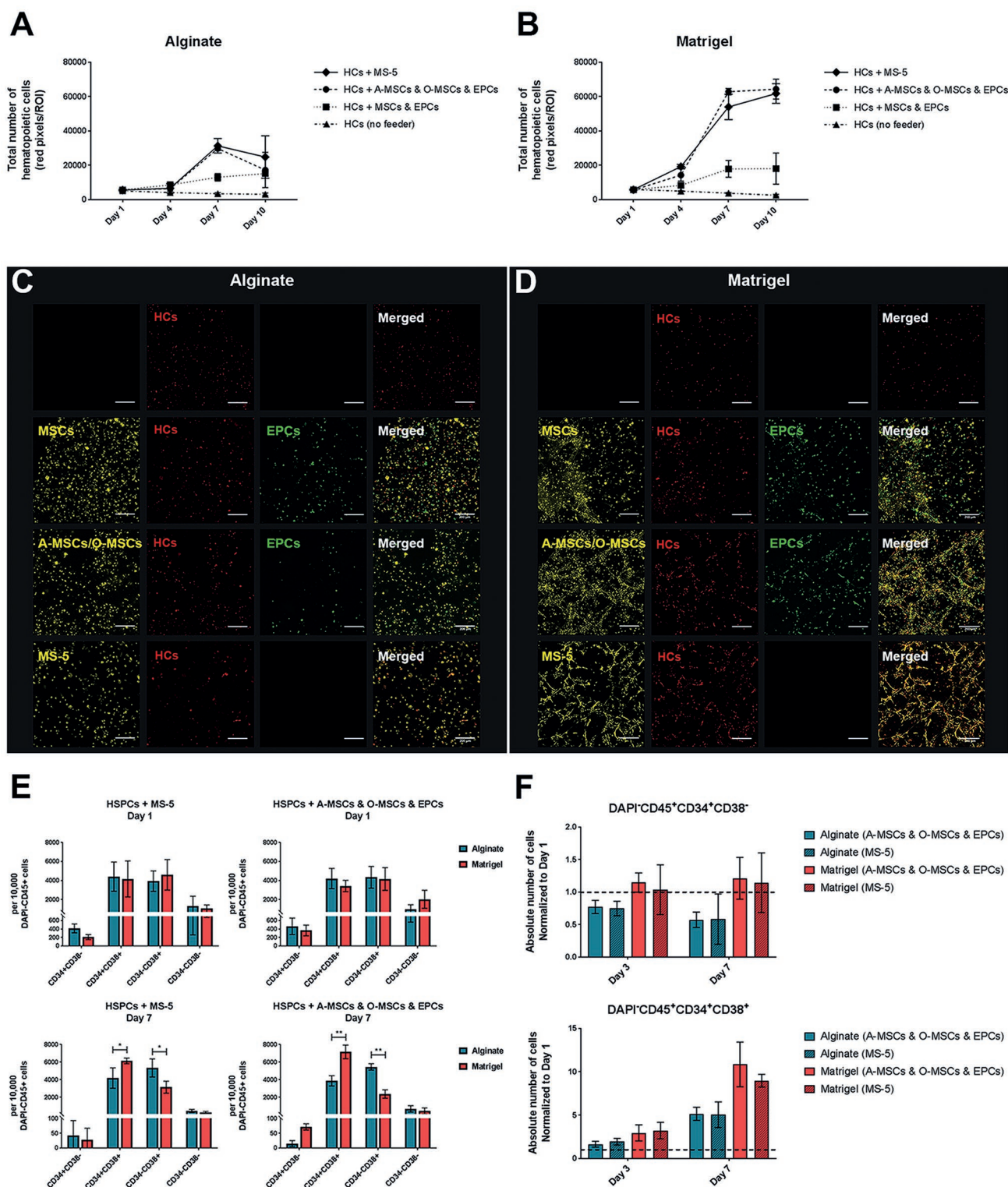


**Figure 3.** Comparison of the various coculture conditions in both alginate versus Matrigel. HSPC cultures ( $n = 3$ ) were analyzed after 1, 4, 7, and 10 d of (co)culture. A,B) Quantification of the number of HCs cultured in alginate and Matrigel. C,D) Corresponding confocal images after 7 d of coculture in alginate or Matrigel with MSCs, A-MSCs/O-MSCs, or MS-5 cells (DiI, yellow), HCs (DiI, red), and EPCs (DiO, green). The scale bars represent 200  $\mu\text{m}$ . E) Quantification of CD34<sup>+</sup>CD38<sup>-</sup>, CD34<sup>+</sup>CD38<sup>+</sup>, CD34<sup>-</sup>CD38<sup>+</sup>, and CD34<sup>-</sup>CD38<sup>-</sup> cells within the DAPI<sup>+</sup>CD45<sup>+</sup> population after A-MSCs/O-MSCs/EPCs and MS-5 coculture for 1 or 7 d in either alginate or Matrigel. F) Absolute number of CD34<sup>+</sup>CD38<sup>-</sup> and CD34<sup>+</sup>CD38<sup>+</sup> cells in culture, normalized to their initial seeded number at day 1, supported by A-MSCs/O-MSCs/EPCs or MS-5 in either alginate or Matrigel. Data are presented as mean  $\pm$  SD. \*  $p < 0.05$ , \*\*  $p < 0.01$ .

(Figure 3E). Alginate showed an increase in the more differentiated CD34<sup>+</sup>CD38<sup>+</sup> population at day 7. When analyzing absolute cell numbers, Matrigel cultures maintained CD34<sup>+</sup>CD38<sup>-</sup> HSPCs during 7 d of culture, and enhanced CD34<sup>+</sup>CD38<sup>+</sup> HSPCs compared to their initial numbers (Figure 3F). The supporting cells cultured in Matrigel were capable of forming networks through cell–cell contact. When cultured in alginate, cells had a rounded phenotype with no visible cell–cell contact during all time points (1, Supporting Information). Matrigel facilitated cell–cell interactions, supporting the development of a differentiated hematopoietic population as well as the maintenance of immature multipotent hematopoietic progenitors.

#### 2.4. HCs Colocalize with Supporting Cells in 3D Matrigel

To look at cell–cell interactions during coculture, the Matrigel-based cultures were analyzed further. After 1 or 4 d of culture, round cells evenly distributed throughout the gel. From day 7 onwards, the stromal cells self-assembled, forming networks throughout the Matrigel (data not shown). Clusters of HCs always colocalized with the supporting networks. In the primary cell conditions (MSCs/EPCs or A-MSCs/O-MSCs/EPCs), HC clusters were present in luminal structures at day 14 (Figure 4A,B). MS-5 did not form similar luminal structures (Figure 4C).

The preferential colocalization of HCs with either CD31<sup>+</sup> endothelial cells, or CD31<sup>-</sup> mesenchymal cells was also analyzed. Direct colocalization of HCs with MSCs (differentiated or nondifferentiated) as well as colocalization with CD31<sup>+</sup> cells was observed (Figure 5A–C). Larger clusters of HCs were found colocalizing with MSCs. This was also observed when staining for CD34<sup>+</sup>, larger clusters of CD34<sup>+</sup> HSPCs colocalized with differentiated MSCs. However, also CD34<sup>+</sup> EPCs could be identified in close proximity to the CD34<sup>+</sup> HSPCs (Figure 5D).

The morphology of the cultured CD31<sup>+</sup> EPCs changed under the influence of cocultured HCs. When cultured only with MSCs, long combined networks of MSCs and EPCs developed. When cocultured with HCs, elongated CD31<sup>+</sup> EPCs were observed, as well as round, sinusoidal-like CD31<sup>+</sup> cell clusters (Figure 5A–C).

#### 2.5. The Addition of Hematopoietic Cytokines Does Not Improve HSPC Maintenance in Primary Cell Cocultures

The primary cell cocultures (in absence or presence of feeder cells (i.e., MSCs/EPCs, A-MSCs/O-MSCs/EPCs, MS-5)) were performed with or without FBS, and with or without additional cytokines (TPO (20 ng mL<sup>-1</sup>), SCF (50 ng mL<sup>-1</sup>), FLT-3 (50 ng mL<sup>-1</sup>), IL-3 (20 ng mL<sup>-1</sup>), and IL-6 (10 ng mL<sup>-1</sup>)). At day 10, cytokine supplementation (in medium with or without fetal bovine serum (FBS)) increased the CD34<sup>+</sup> cell population in absence of feeder cells. In absence or presence of FBS, this number could be significantly increased further with the addition of either MSCs/EPCs, A-MSCs/O-MSCs/EPCs, or MS-5. No significant differences in the CD34<sup>+</sup> population were

observed in presence or absence of additional cytokines, using feeder cells (Figure 6A). Also, the colony-forming potential of HSPCs was similar after culture with or without cytokines (Figure 6B).

In absence of FBS, a decreased total number of CD34<sup>+</sup> cells was observed in the presence of primary feeder cells (MSCs/EPCs, A-MSCs/O-MSCs/EPCs, or MS-5), however, there were still significantly more CD34<sup>+</sup> cells than when cultured without feeder cells. No significant differences were observed in the presence or absence of additional cytokines (Figure 6A). No effect of the added FBS was seen on the support of HSPCs in vitro, as the HSPCs cultured without feeder cells (in the presence of FBS) did not show a sustained CD34<sup>+</sup> population at day 10. This is in contrast to the HSPCs cultured without feeder cells but with additional cytokines (Figure 6A). Looking at the morphology of the supporting primary cells with or without FBS, clear differences were observed (Figure 6C). No supportive networks developed in the cultures without FBS, suggesting an affected supporting cell population, needed to support the CD34<sup>+</sup> population in vitro.

These results show that the primary coculture model optimally performs when cultured in FBS supplemented medium, which does not support CD34<sup>+</sup> HSPCs by itself, without the need of additional supportive cytokines for HSPC survival and maintenance.

#### 2.6. Hypoxic Environment Present within 3D Culture without Compromising Cellular Viability, Proliferation, or Morphology

The primary cell-based coculture model was further characterized in regard to hypoxia development taking into account different volumes of the model (30 or 50  $\mu$ L). The HSPC cocultures, cultured under standard conditions (normoxic condition), cultured with a chemical inducer of hypoxia (hypoxic condition), or cultured with a synthetic oxygen carrier (hyperoxic condition), were analyzed for cell survival, proliferation, and the presence of cellular hypoxia, using hypoxia marker pimonidazole.

Viable supporting cells (MSCs/EPCs) were observed in all three conditions, during 14 d of culture. However, morphological differences were observed in the hypoxia-induced condition (Figure 7A), with decreasing numbers over time. The normoxic cocultures showed higher cell proliferation compared to the hypoxic cocultures but less than the hyperoxic cocultures (Figure 7A,B). A clear difference in hypoxia generated was seen through the staining of pimonidazole. Hypoxia was present in both the hypoxic and normoxic cultured hydrogel cocultures, with very low levels of expression in the hyperoxic cocultures (Figure 7C,D). Similar results were obtained for A-MSCs/O-MSCs/EPCs (data not shown). The level of hypoxia can be reduced or increased in the 3D model, by changing the volume of the culture, or through addition of a synthetic oxygen carrier.

The results show the development of a hypoxic environment within the HSPC bone marrow model when cultured in a conventional incubator. The hypoxic environment does not compromise the viability, proliferation, or morphology of the supporting cells.

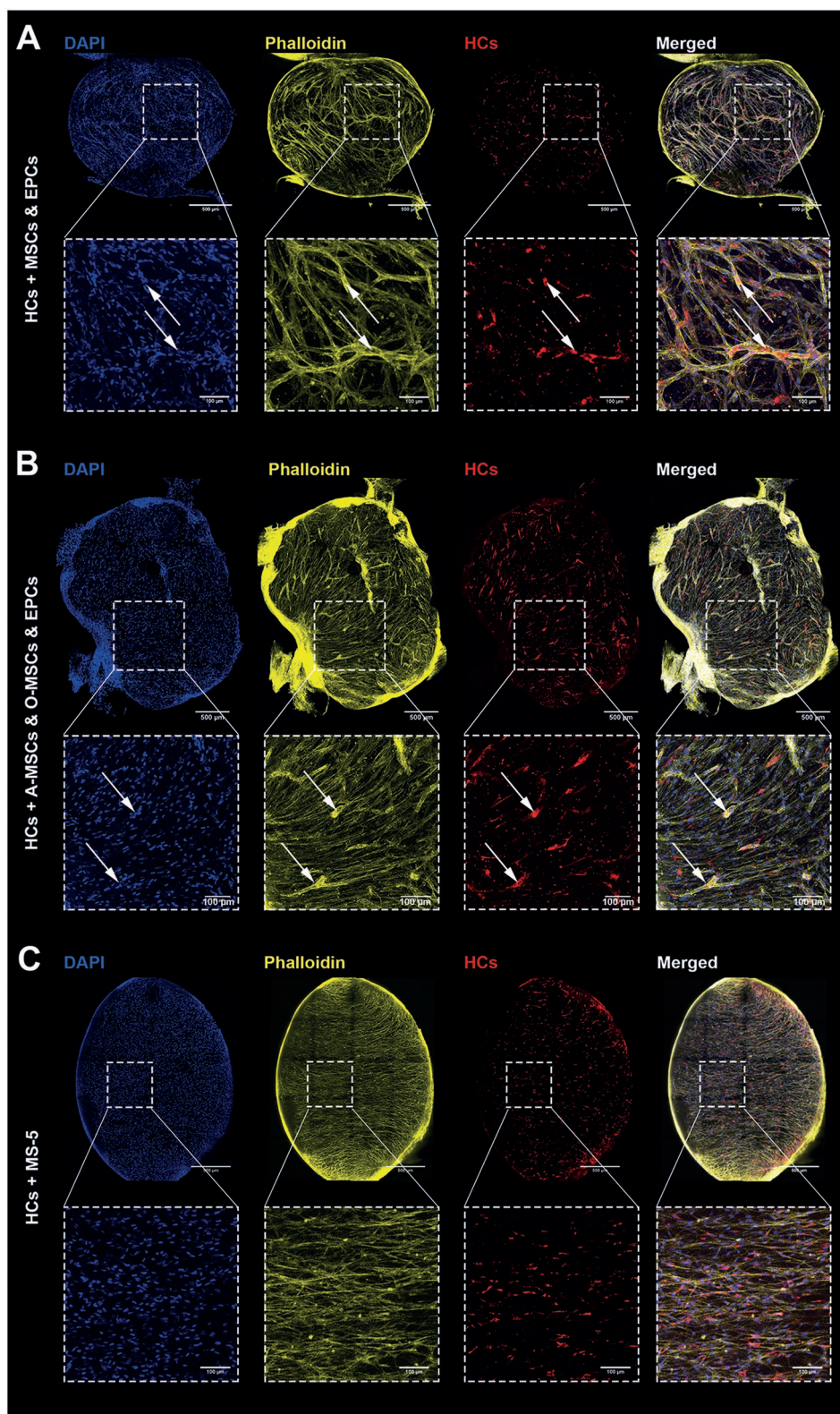


**Figure 4.** Complete overviews of the HSPC niche models after 14 d of culture in Matrigel. A,B) Confocal overview images showing the undifferentiated primary HSPC niche model and differentiated primary HSPC niche model. Stromal networks have been formed, containing luminal structures (zoomed images, white dashed squares, white arrows) with colocalizing HCs. C) Confocal overview images of MS-5 coculture. MS-5 appears as structured networks throughout the culture. No luminal structures were observed (zoomed images, white dashed squares). HCs colocalize with MS-5 networks. DAPI (blue), F-actin (phalloidin, yellow), and HCs (DiD, red). The scale bars represent 500  $\mu\text{m}$  (overviews) or 100  $\mu\text{m}$  (zoomed images).

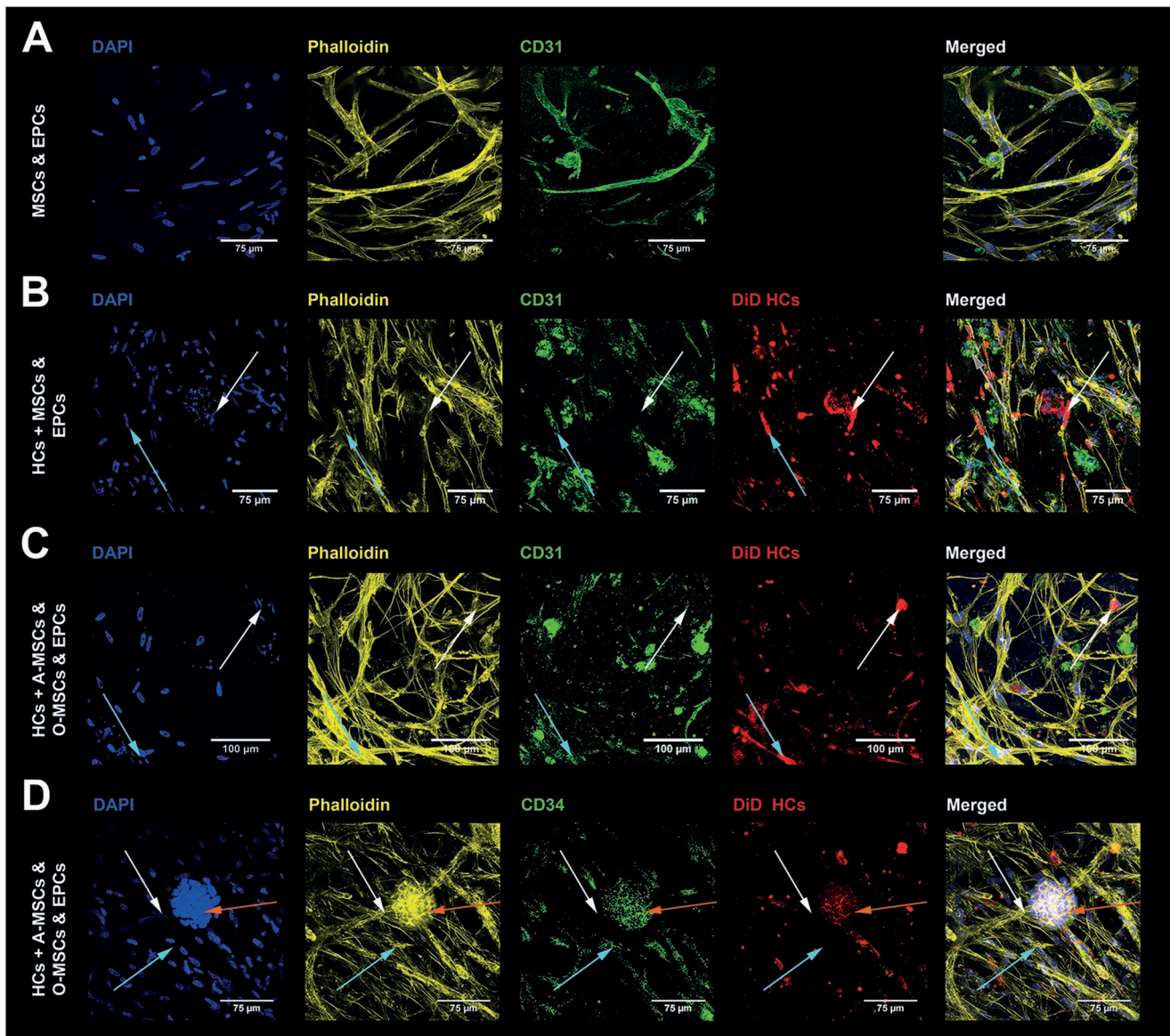


**Figure 5.** HC localization with and morphology of endothelial structures. Confocal images of CD31<sup>+</sup> EPCs (green and yellow) and MSCs (yellow only) cultured A) without HCs and B) with HCs (red), or C) CD31<sup>+</sup> EPCs (green and yellow) and A-MSC/O-MSCs (yellow only) with HCs (red). Combined networks of MSCs or A-MSCs/O-MSCs and EPCs can be observed. The CD31<sup>+</sup> EPCs appeared in round cell clusters or elongated within the stromal networks, when grown together with HCs. Without HCs, mainly elongated structures were observed. HC clusters can be found colocalizing with either MSCs or A-MSCs/O-MSCs (white arrows) or with CD31<sup>+</sup> EPCs (cyan arrows). D) CD34<sup>+</sup> HSPCs (green and red, orange arrows) can also be found in close proximity to both CD34<sup>+</sup> EPCs (cyan arrows) or A-MSCs/O-MSCs (white arrows), DAPI (blue), F-actin (phalloidin, yellow), CD31 or CD34 (green), and HCs (DiD, red). The scale bars represent 75  $\mu\text{m}$  (A, B, D) or 100  $\mu\text{m}$  (C).

### 3. Discussion

The developed HSC niche model enables the culture of HSPCs in vitro, using primary human cells that form the main cellular components of the HSC niche.<sup>[40]</sup> The model allows further study of interactions between various supportive cell types and HSPCs. Current 3D models are based on MSCs and/or O-MSCs, mimicking only the endosteal niche.<sup>[24–29,32–37]</sup> MSCs as well as adipogenic and osteogenic progenitors are known to be an essential component of the HSC niche, required for the quiescence, proliferation, and differentiation of HSPCs.<sup>[41,42]</sup>

Also endothelial cells have been shown to play a key role in the regulation of HSPCs, expressing high levels of major niche factors.<sup>[40,43]</sup> Even though quiescent HSCs have been identified preferentially near the perivascular niche,<sup>[12]</sup> this environment is not mimicked in previously developed in vitro HSC niche models. Our model contains a heterogeneous mix of primary cells that do not require the addition of cytokines to the 3D culture to support HSPCs.

The ECM of the stem cell niche has been shown to have an important instructive role, as it can directly or indirectly modulate the residing stem cells.<sup>[19]</sup> This has been confirmed by

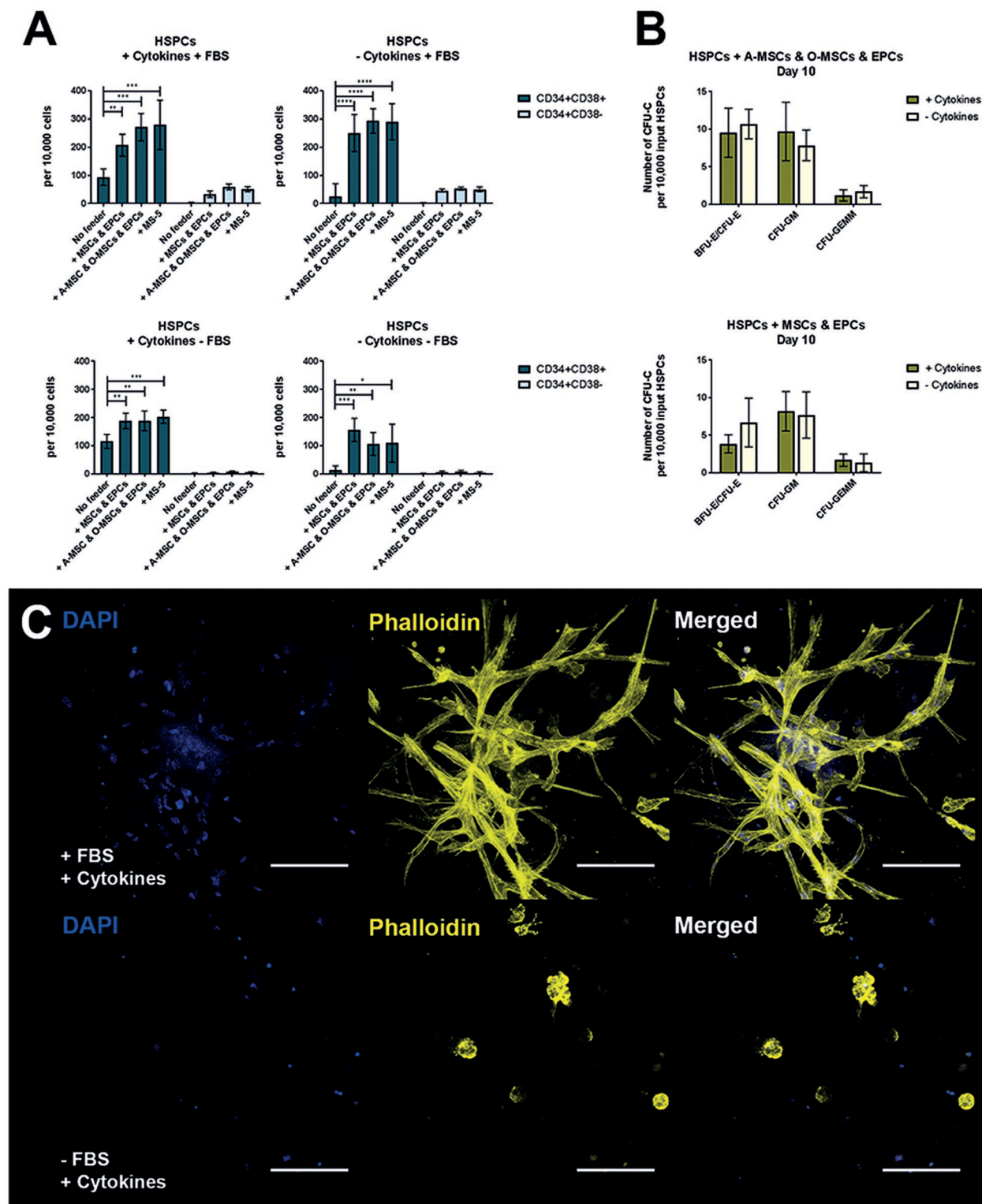


**Figure 6.** Varying medium composition effects on HSPC survival within the HSPC niche models. Each cellular condition ( $n = 3$ ) was cultured either with or without FBS, and with or without cytokines (TPO ( $20 \text{ ng mL}^{-1}$ ), SCF ( $50 \text{ ng mL}^{-1}$ ), FLT-3 ( $50 \text{ ng mL}^{-1}$ ), IL-3 ( $20 \text{ ng mL}^{-1}$ ), and IL-6 ( $10 \text{ ng mL}^{-1}$ )). Results are shown after day 10 of culture. A) Quantification of  $\text{CD34}^+\text{CD38}^+$  and  $\text{CD34}^+\text{CD38}^-$  cells in absence of feeder, or with MSCs/EPCs, A-MSCs/O-MSCs/EPCs, or MS-5 for each culture condition. B) Quantification of colony-forming cells (BFU-E, CFU-GM, or CFU-GEMM) in the two primary cell conditions (MSCs/EPCs or A-MSCs/O-MSC/EPCs) containing FBS, with or without cytokines. C) Confocal images showing A-MSCs/O-MSCs/EPCs (phalloidin (yellow), DAPI (blue)) cultured with and without FBS on day 10, representative for the other stromal coculture conditions. Data are presented as mean  $\pm$  SD. \*  $p < 0.05$ , \*\*  $p < 0.01$ , \*\*\*  $p < 0.001$ , \*\*\*\*  $p < 0.0001$ . The scale bars represent  $150 \mu\text{m}$ .

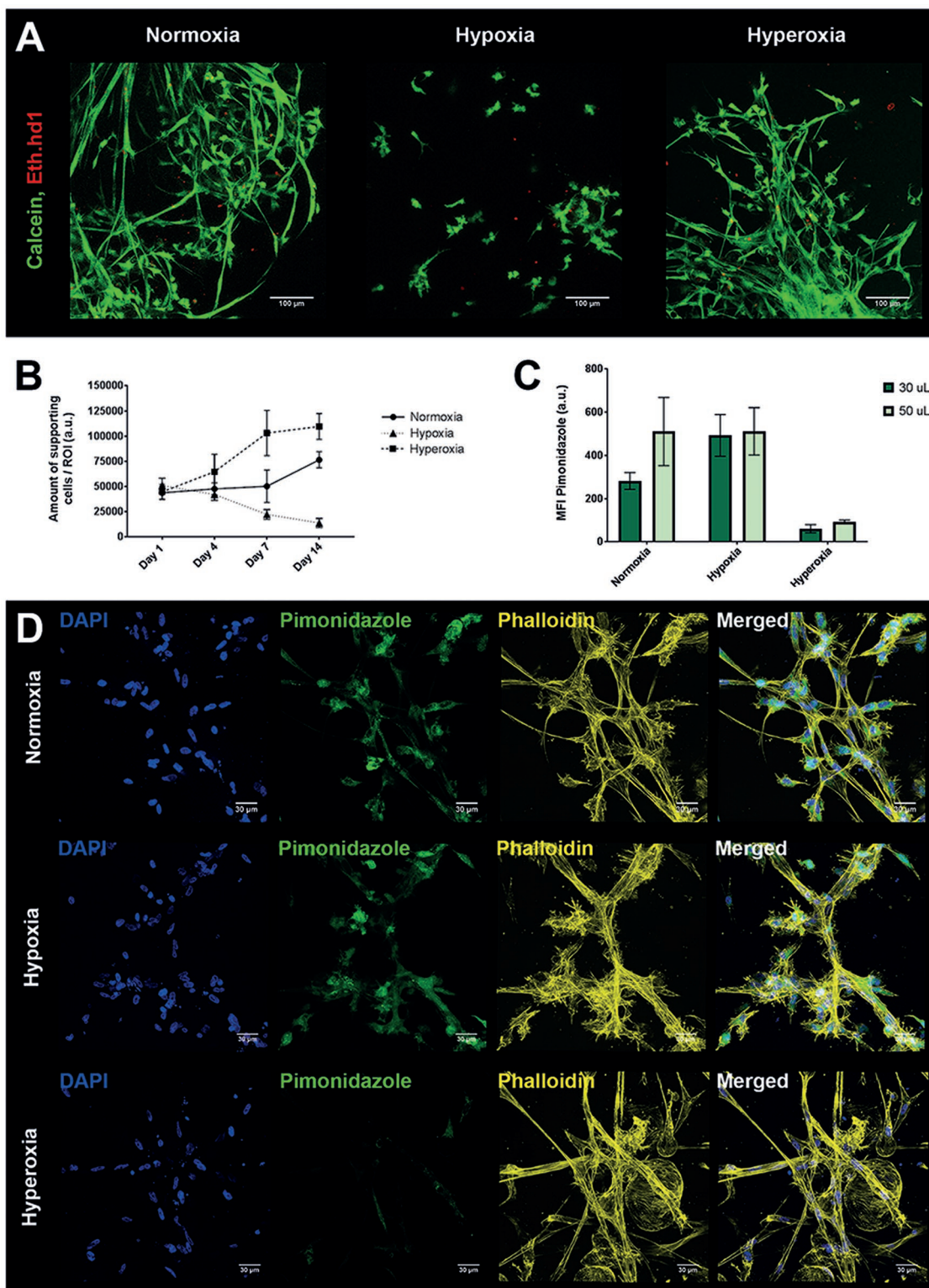


**Figure 7.** Characterization of hypoxia within the HSPC niche model. 3D cultured MSCs/EPCs, in a conventional incubator (37 °C; 5% CO<sub>2</sub>) either without (normoxia) or with 100 µm cobalt (II) chloride hexahydrate (CoCl<sub>2</sub>, hypoxia) or 10% (w/v) synthetic oxygen carrier perfluorotributylamine (PFTBA, hyperoxia). A) Confocal images showing alive (green) and dead (red) cells at day 14 in 50 µL plugs. B) Amount of supporting MSCs/EPCs over time in 50 µL plugs. C) Mean fluorescent intensity of pimonidazole (hypoxia marker) at day 14 in both 30 and 50 µL plugs, with D) the corresponding confocal images at day 14 in both 50 µL plugs. DAPI is shown in blue, hypoxia in green (pimonidazole), and F-actin in yellow (phalloidin). Data are presented as mean ± SD. The scale bars represent 30 µm.

using different ECM mimicking hydrogels, where various supportive effects of the materials were observed toward the cultured HSPCs.<sup>[22,33]</sup> This ECM effect was taken into account by testing different hydrogels as a supportive material, comparing both alginate, lacking cell-adhesive components, and Matrigel, containing abundant cell-adhesive components, for their performance in an in vitro HSPC model. Both hydrogels facilitated a continuous presence of immature colony-forming hematopoietic progenitors, suggesting sufficient trophic factors excreted by the supporting cell population for their in vitro support. The used hydrogels by themselves did not have a supportive effect on the cultured HSPCs, as these immature hematopoietic progenitors could not be maintained without feeder cells in either alginate or Matrigel. The presence of ECM proteins and remaining growth factors in the growth factor reduced Matrigel did facilitate the proliferation of CD34<sup>+</sup>CD38<sup>+</sup> hematopoietic cells to a higher extent than observed in alginate, and better maintained the CD34<sup>+</sup>CD38<sup>-</sup> population during 7 d. In alginate, a higher increase in the more differentiated CD34<sup>-</sup>CD38<sup>+</sup> was observed.

The use of Matrigel enabled the stromal cells to reassemble, forming dense networks. The formation of networks is indicative for the formation of cadherin-mediated intercellular junctions. Single cells without cell–cell interaction maintain a rounded morphology, whereas cells interacting through intercellular junctions display a spread morphology and develop F-actin positive stress fibers, regardless of substrate stiffness or cell–matrix interactions. These intercellular junctions are important for both tissue remodeling and differentiation.<sup>[44]</sup> Especially for endothelial cells these morphological changes are important, as their spread and elongation is associated not only with differentiation and proliferation but also the formation of a functional vascular network.<sup>[45]</sup>

The formation of these cell–cell and cell–matrix interactions limited the ability to decrosslink the culture over time for subsequent analysis. Enzymatic digestion using dispase was used previously to recover cells from Matrigel,<sup>[24]</sup> however, the dispase disturbed the cell surface receptors. Cell recovery solution was capable to depolymerize the Matrigel up to day 10 of culture, which allowed flow cytometry analysis. The analysis of cocultures at later time points was only possible using confocal imaging. To distinguish the cultured HSPCs from the supporting cells, lipophilic tracers were used, enabling both live cell imaging over time and analysis of fixated cultures as a whole. At day 0, a lineage depleted HSPC population was stained with DiD. During culture, the composition of this heterogeneous cell population was shown to change over time. Additional analyses are needed to confirm the presence of either colony-forming or CD34<sup>+</sup> HSPCs within the traced hematopoietic population, also taking in account possible dye transfer from one cell type to the other.<sup>[46]</sup>

The cellular compartment of the model was optimized using relevant cell types of both the perivascular and endosteal niche.<sup>[10,11]</sup> MSCs, A-MSCs, O-MSCs, and EPCs were cultured alone, or in various ratios of cells combined for the cocultures. The model was compared to a stromal feeder cell line (MS-5) traditionally used to support HSPCs in vitro.<sup>[13–15]</sup> Recently, developed models have shown functionality of their 3D endosteal environment comparing them to controls with

no traditional feeder cells. Instead, these models applied cell types that are suboptimal for in vitro HSPC culture, such as 2D cultured MSCs and/or O-MSC.<sup>[25,28]</sup> Also cytokine supplemented media was used,<sup>[27,32,33]</sup> with less supportive capacities toward primitive HSPCs over time when compared to feeder cell lines.<sup>[47]</sup> Other studies focused on optimizing hydrogels or culture conditions did not include controls containing supportive cells or cytokines other than the ones tested in their endosteal models.<sup>[22,24,36]</sup> A direct comparison of culture conditions and components required for the maintenance of HSPC is preferred, in order to evaluate the supportive potential of experimental conditions in newly developed in vitro HSC niche models.

The presence of MSCs or O-MSCs in our model offered less support toward colony-forming HSPCs than MS-5 cells, yet MSCs or O-MSCs were used in recent primary cell models.<sup>[24–29,32–37]</sup> Also, A-MSC or EPCs alone showed less supportive capacities. The ability of these primary human cells to support HSPCs increased when combining them. The optimal condition contained A-MSCs, O-MSCs, and EPCs. Since MSCs, a heterogeneous cell population, are known to not differentiate uniformly during 14 d, undifferentiated MSCs as well as lineage committed MSCs are expected to be present within this coculture condition.<sup>[48]</sup> The combined primary cells supported the growth of HSPCs, similar to MS-5 cells. However, the usage of primary human cell types offers the possibility to culture HSPCs in an environment closely mimicking the in vivo HSC niche. The supportive function of the HSC niche model does still decline over time, comparable to the decline seen when using MS-5 cells. The main challenge will remain to ensure prolonged maintenance of HSPCs in an in vitro model, and may lay in allowing interaction with various other cell types including immune cells.

The HSC niche model that we developed showed a highly HSPC supportive potential compared to cytokine supplemented HSPCs without feeder cells. The developed model contains various cellular components that do not need further supplementation with common HSPC cytokines. These results indicate that the cellular interactions in the in vitro model mimic at least part of the in vivo complexity, suggesting the formation of a functional in vitro HSC niche. Additionally, the cells residing in the model created a hypoxic niche, an important characteristic of the in vivo HSC niche.<sup>[6,49]</sup> Our model thus mimics important features and characteristics of the natural in vivo HSC niche.

## 4. Conclusions

The developed in vitro HSC niche model provides the possibility to culture HSPCs using primary human cells, without further cytokine supplementation to the culture medium. The combination of differentiated adipogenic, osteogenic, and endothelial cells in Matrigel optimally supports HSPC maintenance as well as hematopoiesis. Using this model, the interactions of HSPCs with varying human microenvironments can be studied, such as interactions between HSPCs and the different cell types of both the endosteal and perivascular niche. The mimicking of these niche elements, and the ability to exclude/include cellular

components or interfere with cell–cell interactions, enables the study of the niche itself, and its active participation in normal hematopoiesis as well as disease pathogenesis.

## 5. Experimental Section

**Primary Cells and Cell Lines:** All primary tissue samples were obtained after written informed consent, and used protocols were approved by the local ethics committee of the University Medical Center Utrecht in accordance with the Declaration of Helsinki.

Umbilical cord blood was obtained from full-term pregnancies. The mononuclear cell (MNC) fraction was isolated by centrifugation using Ficoll-Paque PLUS (GE Healthcare). HSPCs were obtained from the MNCs using the human Lineage Cell Depletion Kit (MACS Miltenyl Biotec). The MACS selection was checked using flow cytometry, reaching an average CD34<sup>+</sup> purity of 70.3% ± 5.1% (Table S1, 2, Supporting Information). The lineage negative population was directly used in coculture experiments and plated in an in vitro colony-forming unit-cell assay (CFU-C assay, day 0).

EPCs were isolated from cord blood and characterized as late outgrowth endothelial progenitor cells (also named endothelial colony-forming cells) as previously described.<sup>[50,51]</sup> EPCs were expanded in EPC medium (EBM-2 Basal Medium (Gibco) supplemented with 10% (v/v) FBS (Gibco), 100 U mL<sup>-1</sup> penicillin, and 100 µg mL<sup>-1</sup> streptomycin (Gibco) and EGM-2 SingleQuots (Lonza)).

MSCs were isolated from bone marrow as described previously.<sup>[52]</sup> MSCs were expanded in MSC medium ( $\alpha$ -minimal essential media ( $\alpha$ MEM, Gibco), 10% (v/v) FBS, 0.2 × 10<sup>-3</sup> M L-ascorbic acid 2-phosphate, 100 U mL<sup>-1</sup> penicillin, and 100 µg mL<sup>-1</sup> streptomycin). MSC differentiation was performed in osteogenic medium (MSC medium supplemented with 10 × 10<sup>-3</sup> M  $\beta$ -glycerophosphate and 10 × 10<sup>-9</sup> M dexamethasone (both Sigma)) or adipogenic medium ( $\alpha$ MEM supplemented with 10% (v/v) FBS, 100 U mL<sup>-1</sup> penicillin and 100 µg mL<sup>-1</sup> streptomycin, 0.5 × 10<sup>-3</sup> M 3-isobutyl-1-methylxanthine (IBMX), 0.2 × 10<sup>-3</sup> M indomethacin, 1.72 × 10<sup>-6</sup> M insulin and 1 × 10<sup>-6</sup> M dexamethasone (all Sigma)) for 14 d before use in coculture experiments. Differentiated MSCs toward the adipogenic or osteogenic lineage are referred to as A-MSC or O-MSC, respectively. To assess differentiation, some cells were fixed with 4% formaldehyde for 15 min at room temperature. The O-MSCs were stained with 2% Alizarin red solution (Sigma) for 5 min. The A-MSCs were incubated for 5 min in 60% isopropanol (Avantor Performance Materials) and stained for 5 min in freshly filtered 0.22 × 10<sup>-6</sup> M Oil Red O solution (Sigma). Images were taken with an Olympus BX60 microscope.

MS-5 cells were cultured in  $\alpha$ MEM, 10% (v/v) FBS, 2 × 10<sup>-3</sup> M L-glutamine, 100 U mL<sup>-1</sup> penicillin, and 100 µg mL<sup>-1</sup> streptomycin.

**Hydrogels:** High-viscosity alginate powder (International Specialty Products) was sterilized with 100% ethanol and UV light for 20 min. It was dissolved at 20 mg mL<sup>-1</sup> in  $\alpha$ MEM and polymerized by 100 × 10<sup>-3</sup> M CaCl<sub>2</sub> (Sigma) in Tris-buffered saline (pH 7.6) for 15 min. Gelatin methacrylate (gelMA) was synthesized by reacting porcine type A gelatin (Sigma) with methacrylic anhydride (Sigma) at 50 °C for 1 h, as previously described.<sup>[53]</sup> Thawed gelMA was dissolved in  $\alpha$ MEM at 40 °C at a concentration of 50 mg mL<sup>-1</sup>, containing photoinitiator Irgacure 2959 (1 mg mL<sup>-1</sup> Ciba, BASF) and cross-linked for 15 min using 365 nm light in a UVP CL-1000L cross-linker. Growth factor-reduced Matrigel with a high concentration of basement membrane matrix (Corning, 354263) was diluted 1:1 adding  $\alpha$ MEM. Matrigel was pipetted in droplets on the bottom of a 24-well suspension culture plate and incubated for 20 min at 37 °C before medium was added. Plugs of 50 µL were made unless stated otherwise. The compressive modulus of the used hydrogels ranged from 1.2 to 2.8 kPa (3, Supporting Information).

**3D Monocultures:** HSPCs ( $n = 3$  independent experiments), MSCs ( $n = 3$ ), and EPCs ( $n = 3$ ) were encapsulated separately in alginate, gelMA, and Matrigel. Gels containing HSPCs were cultured on top of a confluent MS-5 feeder layer. Cell viability was analyzed at different time

points (after 1, 4, and 7 d, using the Live/Dead Viability/Cytotoxicity Kit for mammalian cells according to the manufacturer's protocol (ThermoFisher)). At least 50 cells were scored per condition; double stained cells were scored as dead cells from images taken with an Olympus BX60 microscope.

**3D Cocultures:** HSPCs ( $n = 4$ ) were cocultured with different types of supporting cells in the following mixes and ratios: 6:1 (MSC:HSPC, EPC:HSPC, A-MSC:HSPC, O-MSC:HSPC), 3:3:1 (MSC:EPC:HSPC, A-MSC:EPC:HSPC or O-MSC:EPC:HSPC), or 2:2:2:1 (A-MSCs:O-MSCs:EPCs:HSPC). As a positive control, MS-5 cells were used, cultured in a 6:1 ratio. As a negative control, HSPCs were cultured alone (no feeder) in the hydrogels, at equal numbers compared to the HSPCs of the coculture conditions. The single or cocultured cells were pipetted into a 15 mL tube per condition, the seeding density and absolute number of these conditions are described in Tables S2 and S3 (Supporting Information). After centrifugation, the medium was removed and the entire cell pellet, containing either HSPCs or both HSPCs and supporting cells, was resuspended in either alginate 20 mg mL<sup>-1</sup> or Matrigel 50% (v/v), after which the gel was crosslinked as described above.

HSPCs were cocultured in HSPC medium (Iscove's modified Dulbecco's medium (IMDM, Gibco) supplemented with 10% (v/v) FBS, 100 U mL<sup>-1</sup> penicillin and 100 µg mL<sup>-1</sup> streptomycin, and 2 × 10<sup>-3</sup> M L-glutamine (ThermoFisher)) that was added in an equal ratio to the medium of the cocultured cells (MSC medium, EPC medium, adipogenic medium, and/or osteogenic medium). The cocultures were stopped on day 1, day 3 or 4, day 7, and day 10 for further analysis.

The standard mix medium containing 10% (v/v) FBS, but no additional added cytokines, was also compared to mix medium containing no FBS, or mix medium with or without FBS containing added cytokines: TPO (20 ng mL<sup>-1</sup>), SCF (50 ng mL<sup>-1</sup>), FLT-3 (50 ng mL<sup>-1</sup>), IL-3 (20 ng mL<sup>-1</sup>), and IL-6 (10 ng mL<sup>-1</sup>) (Immunotools). The survival of HSPCs ( $n = 3$ ) in the four different media was compared in four culture conditions: HSPCs, HSPCs/MSCs/EPCs, HSPCs/A-MSCs/O-MSCs/EPCs, and HSPCs/MS-5. The cocultures were stopped on day 1, day 3, day 7, and day 10 and assessed by flow cytometry and CFC assays.

**CFU-C Assay:** Alginate plugs were decrosslinked with a 55 × 10<sup>-3</sup> M sodium citrate solution (Sigma). Matrigel plugs were dissolved using dispase (Corning) according to the manufacturer's protocol. The recovered cells were suspended in methylcellulose-based medium (MethoCult H4435 Enriched, Stem Cell Technologies) and incubated for 14 d after which three different colony types were counted based on their morphology (BFU-E/CFU-E: burst-forming unit-erythroid/colony-forming unit-erythroid, CFU-GM: colony-forming unit-granulocyte, macrophage, CFU-GEMM: colony-forming unit-granulocyte, erythrocyte, macrophage, megakaryocyte).

**Flow Cytometric Characterization:** Alginate plugs were decrosslinked with a 55 × 10<sup>-3</sup> M sodium citrate solution (Sigma), Matrigel plugs were dissolved using Cell Recovery Solution (Corning). The obtained cells were stained with hematopoietic lineage marker antibodies (10:100, FITC anti-human hematopoietic lineages, eBioscience), AF647 anti-CD34 (1:100, Biolegend), PE anti-CD38 (1:100, eBioscience), and PE-Cy7 anti-CD45 (1:100, BD Biosciences). DAPI (100 ng mL<sup>-1</sup>, Biolegend) was added to determine cell death. Flow cytometry analysis was performed using a FACS Canto II (Becton Dickinson).

**Hydrogel Comparison:** The proliferation of HSPCs ( $n = 3$ ) was compared after culture in alginate and Matrigel in absence or presence of different cell type combinations (HSPCs/MSCs/EPCs, HSPCs/A-MSCs/O-MSCs/EPCs, or HSPCs/MS-5). Some cells were labeled with Vybrant Multicolor Cell-Labeling Kit (Invitrogen). Cells were incubated for 20 min at 37 °C with either DiD (HSPCs), DiI (MSCs, A-MSCs, O-MSCs, or MS5), and DiO (EPCs), according to manufacturer's protocol. The stained cultures were imaged over time using live cell imaging (days 1, 4, 7, and 10). The rest of the (unstained) cultured cells were used for CFU-C and flow cytometry analysis at day 1, 4, 7, and 10, as described previously, or fixed with 4% formaldehyde at day 14. The cultures were permeabilized with 0.2% Triton-X 100, stained with phalloidin-TRITC and DAPI (both FAK100 Kit; Merck Millipore) according to the

manufacturer's protocol. All images were taken using a Leica SP8X Laser Scanning Confocal Microscope.

**Normoxic 3D Cocultures Compared to Hypoxic and Hyperoxic Cocultures:** Cobalt (II) chloride hexahydrate (CoCl<sub>2</sub>, Sigma) was used at the final concentration of  $100 \times 10^{-6}$  M in regular cell culture media to induce hypoxia.<sup>[54]</sup> 10% (w/v) synthetic oxygen carrier perfluorotributylamine (PFTBA, Sigma) was added to the Matrigel before cell addition. All cultures were performed in a conventional incubator (37 °C; 5% CO<sub>2</sub>). Plugs of both 30 and 50 μL (Tables S3 and S4, Supporting Information) were made to visualize hypoxia. Hypoxic cells in the cocultures were detected using the Hypoxyprobe-1 HP6-100 Kit (NPI Inc.). Pimonidazole was added to half of the cocultures for 3 h at a final concentration of  $200 \times 10^{-6}$  M before stopping the experiment (at day 1, 4, 7, and 14). Samples were fixed with 4% formaldehyde and cut in half. The cultures were permeabilized with 0.2% Triton-X 100, blocked with 5% PBS/BSA, and incubated with FITC anti-pimonidazole antibody (1:50) overnight at 4 °C. Samples were then washed with PBS and stained with phalloidin-TRITC and DAPI (both FAK100 Kit; Merck Millipore) according to the manufacturer's protocol. The other half of the cultures was live imaged at day 1, 4, 7, and 14 after staining the cells with the Live/Dead Viability/Cytotoxicity Kit for mammalian cells according to the manufacturer's protocol (ThermoFisher). All cultures were analyzed using a Leica SP8X Laser Scanning Confocal Microscope.

**Immunocytochemistry:** Cocultures containing HSPCs(DiD)/MSCs/EPCs or HSPCs(DiD)/A-MSCs/O-MSCs/EPCs were used for immunodetection of CD31 or CD34. At day 14, fixed cultures were incubated with purified anti-human CD31 antibody (10 μg mL<sup>-1</sup>, Clone WM59, Biolegend) or purified anti-human CD34 antibody (10 μg mL<sup>-1</sup>, clone 581, Biolegend) overnight at 4 °C in TBS containing 1 mg mL<sup>-1</sup> BSA, followed by biotinylated sheep anti-mouse (1:200 in TBS/BSA, RPN1001v1; GE Healthcare) overnight at 4 °C, and Alexa Fluor 488 anti-streptavidin (4 μg mL<sup>-1</sup>, S11226; Life Technologies) overnight at 4 °C. Samples were then stained for TRITC anti-phalloidin (1:200) and DAPI (100 ng mL<sup>-1</sup>, both FAK100 Kit; Merck Millipore). Controls were performed with mouse IgG1 monoclonal antibodies (X0931; Dako) used at similar concentrations. Images were taken with a Leica SP8X Laser Scanning Confocal Microscope.

**Confocal Imaging:** Confocal images were taken with a Leica SP8X Laser Scanning Confocal Microscope using a white light laser (470–670 nm) and Leica LASX acquisition software. Hybrid detectors collected the fluorescent signal from fluorochromes at the following wavelengths: calcein (494/500–525) or ethidium homodimer-1 (528/600–640), which were given the pseudocolors green and red, DiO (484/500–540), Dil (549/565–605), and DiD (644/665–705), which were given the pseudocolors green, yellow, and red, DAPI (405/430–480), FITC (488/490–525), phalloidin-TRITC (532/540–575), and DiD (644/665–705), respectively, which were given the pseudocolors blue, green, yellow, and red. All z-stack images were processed using ImageJ 1.51h software to create single maximum projections. Images of large scaffolds were merged using the mosaic function of the Leica LASX software, stitching the images together using smooth and linear blending.

**Statistical Analysis:** All experimental groups were performed in technical triplicates. Results are presented as mean ± standard deviation for the indicated number of donors. *p* values are based on a repeated measurements analysis of variance (two-way ANOVA) for multiple hypothesis using Dunnett's multicomparison post hoc test, or analysis of variance (one-way ANOVA) for multiple hypothesis testing using Tukey's honestly significant difference (HSD) post hoc test. Data analysis was performed using Prism GraphPad Software and IBM SPSS Statistics version 22. In all tests, *p* values < 0.05 were considered statistically significant. \* *p* < 0.05, \*\* *p* < 0.01, \*\*\* *p* < 0.001, \*\*\*\* *p* < 0.0001.

## Supporting Information

Supporting Information is available from the Wiley Online Library or from the author.

## Acknowledgements

This study was supported in part by a Utrecht University Seed Grant (2013) and the Dutch Arthritis Foundation.

## Conflict of Interest

The authors declare no conflict of interest.

## Keywords

3D in vitro models, bone marrow microenvironments, endosteal niches, hematopoietic stem cell maintenance, perivascular niches

Received: November 8, 2018

Revised: March 5, 2019

Published online: April 3, 2019

- [1] S. J. Morrison, D. T. Scadden, *Nature* **2014**, *505*, 327.
- [2] Q. Wei, P. S. Frenette, *Immunity* **2018**, *48*, 632.
- [3] A. Mendelson, P. S. Frenette, *Nat. Med.* **2014**, *20*, 833.
- [4] L. M. Calvi, D. C. Link, *Blood* **2015**, *126*, 2443.
- [5] J. N. Smith, L. M. Calvi, *Stem Cells* **2013**, *31*, 1044.
- [6] J. A. Spencer, F. Ferraro, E. Roussakis, A. Klein, J. Wu, J. M. Runnels, W. Zaher, L. J. Mortensen, C. Alt, R. Turcotte, R. Yusuf, D. Cote, S. A. Vinogradov, D. T. Scadden, C. P. Lin, *Nature* **2014**, *508*, 269.
- [7] T. Morikawa, K. Takubo, *Pflugers Arch.* **2015**.
- [8] A. C. Gomes, T. Hara, V. Y. Lim, D. Herndler-Brandstetter, E. Nevius, T. Sugiyama, S. Tani-Ichi, S. Schlenner, E. Richie, H. R. Rodewald, R. A. Flavell, T. Nagasawa, K. Ikuta, J. P. Pereira, *Immunity* **2016**, *45*, 1219.
- [9] T. Itkin, S. Gur-Cohen, J. A. Spencer, A. Schajnovitz, S. K. Ramasamy, A. P. Kusumbe, G. Ledergor, Y. Jung, I. Milo, M. G. Poulos, A. Kalinkovich, A. Ludin, O. Kollet, G. Shakhar, J. M. Butler, S. Rafii, R. H. Adams, D. T. Scadden, C. P. Lin, T. Lapidot, *Nature* **2016**, *532*, 323.
- [10] M. Zhao, L. Li, *Cell Res.* **2016**, *26*, 975.
- [11] T. Yin, L. Li, *J. Clin. Invest.* **2006**, *116*, 1195.
- [12] L. Ding, S. J. Morrison, *Nature* **2013**, *495*, 231.
- [13] K. Itoh, H. Tezuka, H. Sakoda, M. Konno, K. Nagata, T. Uchiyama, H. Uchino, K. J. Mori, *Exp. Hematol.* **1989**, *17*, 145.
- [14] C. Issaad, L. Croisille, A. Katz, W. Vainchenker, L. Coulombel, *Blood* **1993**, *81*, 2916.
- [15] N. Nishi, R. Ishikawa, H. Inoue, M. Nishikawa, T. Yoneya, M. Kakeda, H. Tsumura, H. Ohashi, K. J. Mori, *Leukemia* **1997**, *11*, 468.
- [16] B. A. Roeklein, B. Torok-Storb, *Blood* **1995**, *85*, 997.
- [17] P. W. Zandstra, E. Conneally, A. L. Petzer, J. M. Piret, C. J. Eaves, *Proc. Natl. Acad. Sci. USA* **1997**, *94*, 4698.
- [18] A. Bennaceur-Griselli, C. Ponderar, V. Schiavon, W. Vainchenker, L. Coulombel, *Blood* **2001**, *97*, 435.
- [19] F. Gattazzo, A. Urciuolo, P. Bonaldo, *Bioch. Biophys. Acta* **2014**, *1840*, 2506.
- [20] K. Fulzele, D. S. Krause, C. Panaroni, V. Saini, K. J. Barry, X. Liu, S. Weinstein, R. Baron, L. Bonewald, J. Q. Feng, M. Chen, L. S. Weinstein, J. Y. Wu, H. M. Kronenberg, D. T. Scadden, P. D. Pajevic, *Blood* **2013**, *121*, 930.
- [21] M. H. Raaijmakers, S. Mukherjee, S. Guo, S. Zhang, T. Kobayashi, J. A. Schoonmaker, B. L. Ebert, F. Al-Shahrour, R. P. Hasserjian, E. O. Scadden, Z. Aung, M. Matza, M. Merckenschlager, C. Lin, J. M. Rommens, D. T. Scadden, *Nature* **2010**, *464*, 852.

- [22] M. J. Cuddihy, Y. Wang, C. Machi, J. H. Bahng, N. A. Kotov, *Small* **2013**, *9*, 1008.
- [23] Y. Yuan, W. Y. Sin, B. Xue, Y. Ke, K. T. Tse, Z. Chen, Y. Xie, Y. Xie, *Transfusion* **2013**, *53*, 2001.
- [24] M. S. V. Ferreira, C. Bergmann, I. Bodensiek, K. Peukert, J. Abert, R. Kramann, P. Kachel, B. Rath, S. Rutten, R. Knuchel, B. L. Ebert, H. Fischer, T. H. Brummendorf, R. K. Schneider, *J. Hematol. Oncol.* **2016**, *9*, 4.
- [25] M. B. Sharma, L. S. Limaye, V. P. Kale, *Haematologica* **2012**, *97*, 651.
- [26] A. Raic, L. Rodling, H. Kalbacher, C. Lee-Thedieck, *Biomaterials* **2014**, *35*, 929.
- [27] P. E. Bourguine, T. Klein, A. M. Paczulla, T. Shimizu, L. Kunz, K. D. Kokkaliaris, D. L. Coutu, C. Lengerke, R. Skoda, T. Schroeder, I. Martin, *Proc. Natl. Acad. Sci. USA* **2018**, *115*, E5688.
- [28] X. Huang, B. Zhu, X. Wang, R. Xiao, C. Wang, *Int. J. Mol. Med.* **2016**, *38*, 1141.
- [29] J. Tan, T. Liu, L. Hou, W. Meng, Y. Wang, W. Zhi, L. Deng, *Cytotechnology* **2010**, *62*, 439.
- [30] J. E. Nichols, J. Cortiella, J. Lee, J. A. Niles, M. Cuddihy, S. Wang, J. Bielitzki, A. Cantu, R. Mlcak, E. Valdivia, R. Yancy, M. L. McClure, N. A. Kotov, *Biomaterials* **2009**, *30*, 1071.
- [31] Y. Hirabayashi, Y. Hatta, J. Takeuchi, I. Tsuboi, T. Harada, K. Ono, W. R. Glomm, M. Yasuda, S. Aizawa, *Exp. Biol. Med.* **2011**, *236*, 1342.
- [32] I. Leisten, R. Kramann, M. S. V. Ferreira, M. Bovi, S. Neuss, P. Ziegler, W. Wagner, R. Knuchel, R. K. Schneider, *Biomaterials* **2012**, *33*, 1736.
- [33] M. S. Ferreira, W. Jahnen-Dechent, N. Labude, M. Bovi, T. Hieronymus, M. Zenke, R. K. Schneider, S. Neuss, *Biomaterials* **2012**, *33*, 6987.
- [34] P. Wuchter, R. Saffrich, S. Giselbrecht, C. Nies, H. Lorig, S. Kolb, A. D. Ho, E. Gottwald, *Cell Tissue Res.* **2016**, *364*, 573.
- [35] A. P. de Barros, C. M. Takiya, L. R. Garzoni, M. L. Leal-Ferreira, H. S. Dutra, L. B. Chiarini, M. N. Meirelles, R. Borojevic, M. I. Rossi, *PLoS One* **2010**, *5*, e9093.
- [36] L. Rodling, I. Schwedhelm, S. Kraus, K. Bieback, J. Hansmann, C. Lee-Thedieck, *Sci. Rep.* **2017**, *7*, 4625.
- [37] D. Jing, A. V. Fonseca, N. Alakel, F. A. Fierro, K. Muller, M. Bornhauser, G. Ehninger, D. Corbeil, R. Ordemann, *Haematologica* **2010**, *95*, 542.
- [38] L. Ding, T. L. Saunders, G. Enikolopov, S. J. Morrison, *Nature* **2012**, *481*, 457.
- [39] D. L. Glettig, D. L. Kaplan, *Biores. Open Access* **2013**, *2*, 179.
- [40] N. Asada, S. Takeishi, P. S. Frenette, *Int. J. Hematol.* **2017**, *106*, 45.
- [41] S. Mendez-Ferrer, T. V. Michurina, F. Ferraro, A. R. Mazloom, B. D. Macarthur, S. A. Lira, D. T. Scadden, A. Ma'ayan, G. N. Enikolopov, P. S. Frenette, *Nature* **2010**, *466*, 829.
- [42] Y. Omatsu, T. Sugiyama, H. Kohara, G. Kondoh, N. Fujii, K. Kohno, T. Nagasawa, *Immunity* **2010**, *33*, 387.
- [43] S. Rafii, R. Mohle, F. Shapiro, B. M. Frey, M. A. Moore, *Leuk. Lymphoma* **1997**, *27*, 375.
- [44] T. Yeung, P. C. Georges, L. A. Flanagan, B. Marg, M. Ortiz, M. Funaki, N. Zahir, W. Ming, V. Weaver, P. A. Janmey, *Cell Motil. Cytoskeleton* **2005**, *60*, 24.
- [45] K. Tsuji-Tamura, M. Ogawa, *Inflammation Regener.* **2018**, *38*, 25.
- [46] T. P. Lehmann, W. Juzwa, K. Filipiak, P. Sujka-Kordowska, M. Zabel, J. Glowacki, M. Glowacki, P. P. Jagodzinski, *Mol. Med. Rep.* **2016**, *14*, 4529.
- [47] A. Bennaceur-Griscelli, C. Tourino, B. Izac, W. Vainchenker, L. Coulombel, *Blood* **1999**, *94*, 529.
- [48] M. Pevsner-Fischer, S. Levin, D. Zipori, *Stem Cell Rev.* **2011**, *7*, 560.
- [49] C. Nombela-Arrieta, G. Pivarnik, B. Winkel, K. J. Canty, B. Harley, J. E. Mahoney, S. Y. Park, J. Lu, A. Protopopov, L. E. Silberstein, *Nat. Cell Biol.* **2013**, *15*, 533.
- [50] M. V. J. Braham, M. C. Minnema, T. Aarts, Z. Sebestyen, T. Straetemans, A. Vyborova, J. Kuball, F. C. Oner, C. Robin, J. Alblas, *Oncoimmunology* **2018**, *7*, e1434465.
- [51] M. T. Poldervaart, H. Gremmels, K. van Deventer, J. O. Fledderus, F. C. Oner, M. C. Verhaar, W. J. Dhert, J. Alblas, *J. Controlled Release* **2014**, *184*, 58.
- [52] M. V. J. Braham, T. Ahlfeld, A. R. Akkineni, M. C. Minnema, W. J. A. Dhert, F. C. Oner, C. Robin, A. Lode, M. Gelinsky, J. Alblas, *Tissue Eng., Part C* **2018**, *24*, 300.
- [53] W. Schuurman, P. A. Levett, M. W. Pot, P. R. van Weeren, W. J. A. Dhert, D. W. Hutmacher, F. P. W. Melchels, T. J. Klein, J. Malda, *Macromol. Biosci.* **2013**, *13*, 551.
- [54] D. Wu, P. Yotnda, *J. Visualized Exp.* **2011**, 3357.